Journal of Molecular Structure 1238 (2021) 130461

Contents lists available at ScienceDirect

Journal of Molecular Structure

journal homepage: www.elsevier.com/locate/molstr

Crystal structure, MEP/DFT/XRD, thione ⇔ thiol tautomerization, thermal, docking, and optical/TD-DFT studies of (E)-methyl 2-(1-phenylethylidene)-hydrazinecarbodithioate ligand

Ahmed Boshaala[a,*], Musa A. Said[b], Eman A. Assirey[b], Zainab S. Alborki[c], Abeer A. AlObaid[d], Abdelkader Zarrouk[e], Ismail Warad[f,*]

[a] Libya Authority for Scientific Research, Tripoli, Libya
[b] Chemistry Department, College of Science, Taibah University P.O. Box 344, Al-Madinah Al-Munawarah, KSA
[c] Chemistry Department, Faculty of Science, Benghazi University, P O Box 1308 Benghazi, Libya
[d] Department of Chemistry, College of Science, King Saud University, P.O. Box 2455, Riyadh 11451, Saudi Arabia
[e] Laboratory of Materials, Nanotechnology, and Environment, Mohammed V University, Faculty of Sciences, 4Av. Ibn Battuta, PO B.P. 1014 Rabat, Morocco
[f] Department of Chemistry and Earth Sciences, PO Box 2713, Qatar University, Doha, Qatar

ARTICLE INFO

Article history:
Received 6 March 2021
Revised 31 March 2021
Accepted 5 April 2021
Available online 13 April 2021

Keywords:
Schiff base
DFT
Thermal
XRD
Docking
Alzheimer's disease
Donepezil

ABSTRACT

As small-molecule (E)-methyl 2-(1-phenylethylidene)hydrazinecarbodithioate has been prepared and characterized by X-ray single-crystal analysis. In order to elucidate the nature of the intermolecular interactions in the structural lattice, the Hirshfeld surface analysis (HSA) calculation was correlated to the XRD-packing result. Moreover, the XRD bond lengths and angles were compared to their DFT/B3LYP/6-311G(d,p) relative parameters. Considering the thione isomer as a kineticly favoured isomer, the single proton intra-migration from H-N to form S-H thionethiol tautomerization process was successfully computed via QST2 model. Additionally, Mulliken Atomic Charge (MAC), Natural Population Analysis (NPA), and Molecular Electrostatic Potential (MEP) analyses were carried out to confirm this process. The electron transfer and optical behavior of the ligand in DMSO have been exanimated with TD-DFT and HOMO/LUMO calculations. The thermal behavior of the compound was determined in an open room condition via TG/DTG. The two identified isomers of (E)-methyl 2-(1-phenylethylidene)-hydrazinecarbodithioate (thione and thiol forms) were docked against TcAChE (PDB:1EVE) revealed, conspicuous, different protein–drug structures, however, reflects identical docking scores (−7.2 Kcal/mol each), which is compared to the standard donepezil drug used in this study.

1. Introduction

Schiff Bases with nitrogen and sulfur donor atoms are an interesting class of organic ligands that have attracted great attention in the past century [1,2]. A wide range of biological activities has been reported such as antibacterial, antifungal anticancer, and DNA binding [3–10]. The hydrogen bonding through the imino group has tolerated good chelating in biological application [10]. As ligands, the Schiff bases and their metal complexes are promising leads for synthetic, structural, and electrochemical applications [11–15]. Other applications include health and skincare products and paint manufacturing [16]. S-benzyldithiocarbazate (SBDTC) has been thoroughly investigated [9,15–18], whereas S-methyldithiocarbazate (SMDTC) remains, relatively, open for more research, hence, we were inspired to produce this research paper.

The elaboration of efficient density functional theory (DFT) has commissioned the responsible implementation of large atom number molecules (100 atoms); therefore, it became one of the best quantum methods in computations [16,19–21]. Recently, with the help of XRD and HSA analysis, the optimization structure parameters using DFT-theory was updated and enhanced and acquired more confidence and interconnectedness between the three methods [20–22]. Moreover, it helped in evaluating the convergence of practical measurements from theory simulations [23–25].

Docking of compounds is a good theoretical method for learning the drug-molecular interactions mode for example DNA or other proteins via short interactions [26–30]. Theoretical docking together with experimental results helps to explore inorganic complexes or organic compounds for potential medicine nominees

* Corresponding authors.
E-mail addresses: ahmedboshaala@yahoo.co.uk (A. Boshaala), ismail.warad@qu.edu.qa (I. Warad).

https://doi.org/10.1016/j.molstruc.2021.130461
0022-2860/

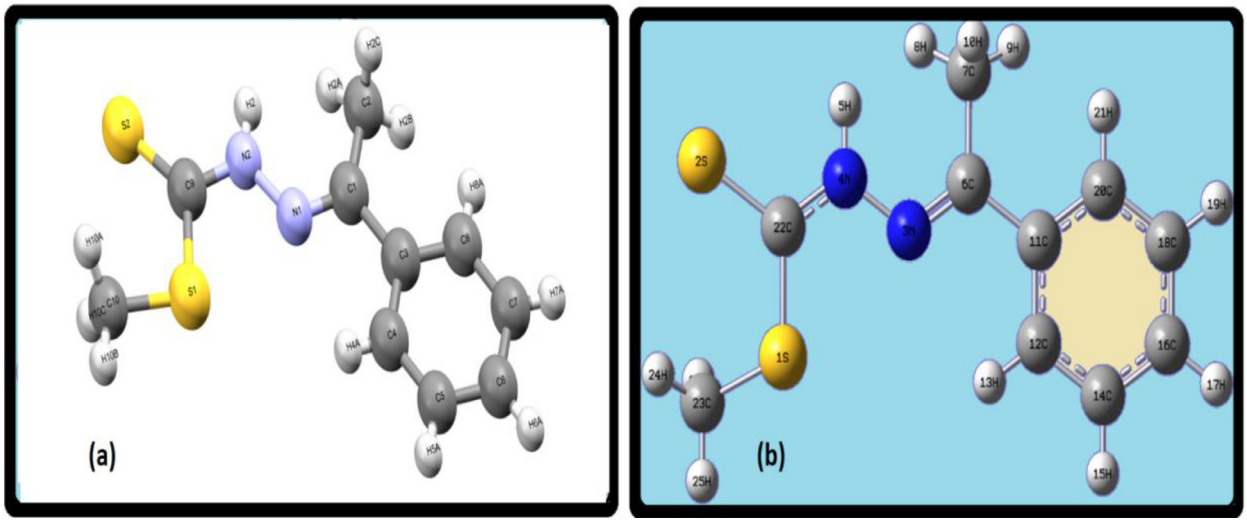

Fig. 1. (a) ORTEP digram, and (b) B3LYP/6–311G(d,p) optimized structure of (E)-methyl 2-(1-phenylethylidene) hydrazinecarbodithioate.

[30]. Alzheimer's disease (AD) is the most common cause of dementia, hence it has received a substantial amount of attention [31]. Cholinesterase inhibitors (ChEIs) are the best-known class of medications that have shown genuine opportunity in treating the functional symptoms of AD [32]. Unfortunately, the approved drugs by the U.S. Food and Drug Administration for Alzheimer's disease which belong to a category of acetylcholinesterase inhibitors were found to have side effects [33], hence the door is widely open for more research. In this research paper, we present a molecular docking study against 1EVE as a leading step towards finding an effective drug for AD and clarify the inhibition mode of the more active compound.

A literature survey of (E)-methyl 2-(1-phenylethylidene) hydrazinecarbodithioate revealed that the XRD and DFT/B3LYP thione⇔thiol tautomrization have not been reported. As a good method, QST2 has been selected for such an intra-migration single proton process. MAC/NPA/MPE-/HSA/XRD-packing analysis helped in understanding the interactions in the crystal lattice. Moreover, the XRD-structure parameters and FT-IR result have been successfully matched to their DFT relative data. The TD-SCF/DFT/B3LYP and HOMO/LUMO calculations were compared to the experimental absorption and Tuac ΔE_g analysis, respectively. The thione andthiol isomers showed low docking score and interesting different protein-ligand structures.

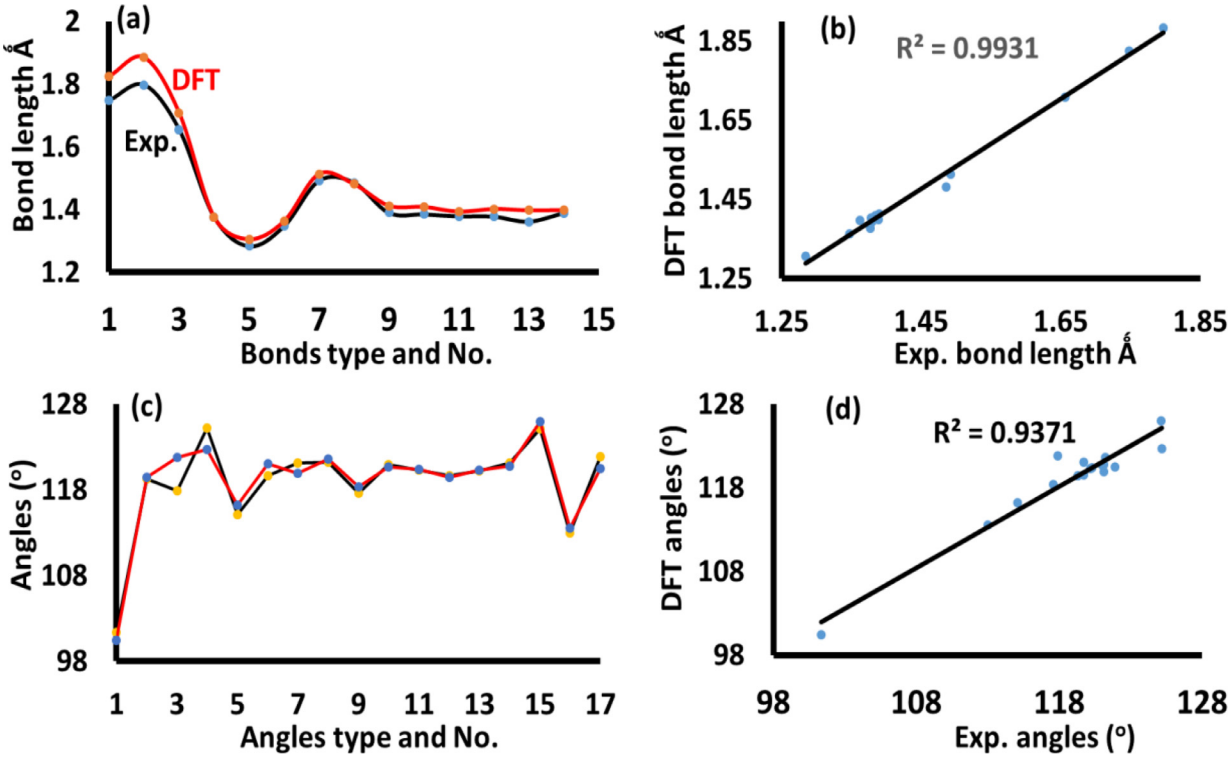

Fig. 2. (a) DFT/XRD bond distances, (b) DF/XRD graphical correlation of bond distances, (c) XRD/DFT angles, and (d) DFT/XRD graphical correlation of the angles.

2. Experimental section

2.1. Materials

All chemicals and solvents were of reagent grade. Chemicals such as hydrazine hydrate (90%); carbon disulfide and potassium hydroxide were purchased from (Fluka-sigma) while benzyl chloride and acetophenone were obtained by Manchester salt and catalysis ltd UK. Methyl iodide wasobtained from FlukaChemica (Switzerland). UV–Vis. measurements were performed in methanol solvent using TU-1901 double-beam spectrophotometer. The FT-IR (MID. 4000–200 cm^{-1}) was recorded in solid state using PerkinElmer Spectrum 1000 FT-IR Spectrometer. The NMR were measured on JOEL 600 MHz spectrometer using $CDCl_3$ solvent.

2.2. (E)-methyl 2-(1-phenylethylidene)hydrazinecarbodithioate

The Schiff base, Methyl(2E)-2-(phenylmethylidene)dithiocarbazate was synthesized by using the procedure [15]. To a solution of SMDTC (5 g, 0.04 mol) in 40 ml of ethanol, 4.8 mL, 0.04 mol of acetophenone was added to the SMDTC mixture. The reaction mixture was refluxing for ~ 3 h, the yellow precipitate was filtrated and washed well by ethanol and dried in desiccator over silica gel to give a crude white product with 6.8 g, 74% yield.

^{1}H NMR (δ_H ppm, $CDCl_3$): 2.1 (s, 3H, CH_3), 2.5 (s, 3H, SCH_3), 7.3 (m, 3H, *p* & *m*-Ph), 2.88 (dd, J = 8.7 Hz, 2H, *o*-Ph), 12.6 (s, 1H, NH). ^{13}C NMR (δ_c ppm, $CDCl_3$): 13.1 (1C, CH_3), 18.2 (1C, SCH_3), 126.2, 128.4 and 138.2 (6C, Ph), 145.8 (1C, C=N), 200.1 (1C, C=S). IR, Ph $\upsilon_{C\text{-}H}$ 3110 cm^{-1}, Me $\upsilon_{C\text{-}H}$ 2940–2880 cm^{-1}, and $\upsilon_{S=C}$ 1030 cm^{-1}, UV–vis. in $CHCl_3$ λ_{max} values at 225, and 312 nm, the m.p 143 °C.

2.3. HSA, and DFT calculation

HSA analysis was performed using CRYSTAL EXPLORER 3.1 program [34]. The DFT-B3LYP 6–311G(d)-computations were carried out in gaseous phase at DFT/B3LYP level of theory using Gaussian09 software [35].

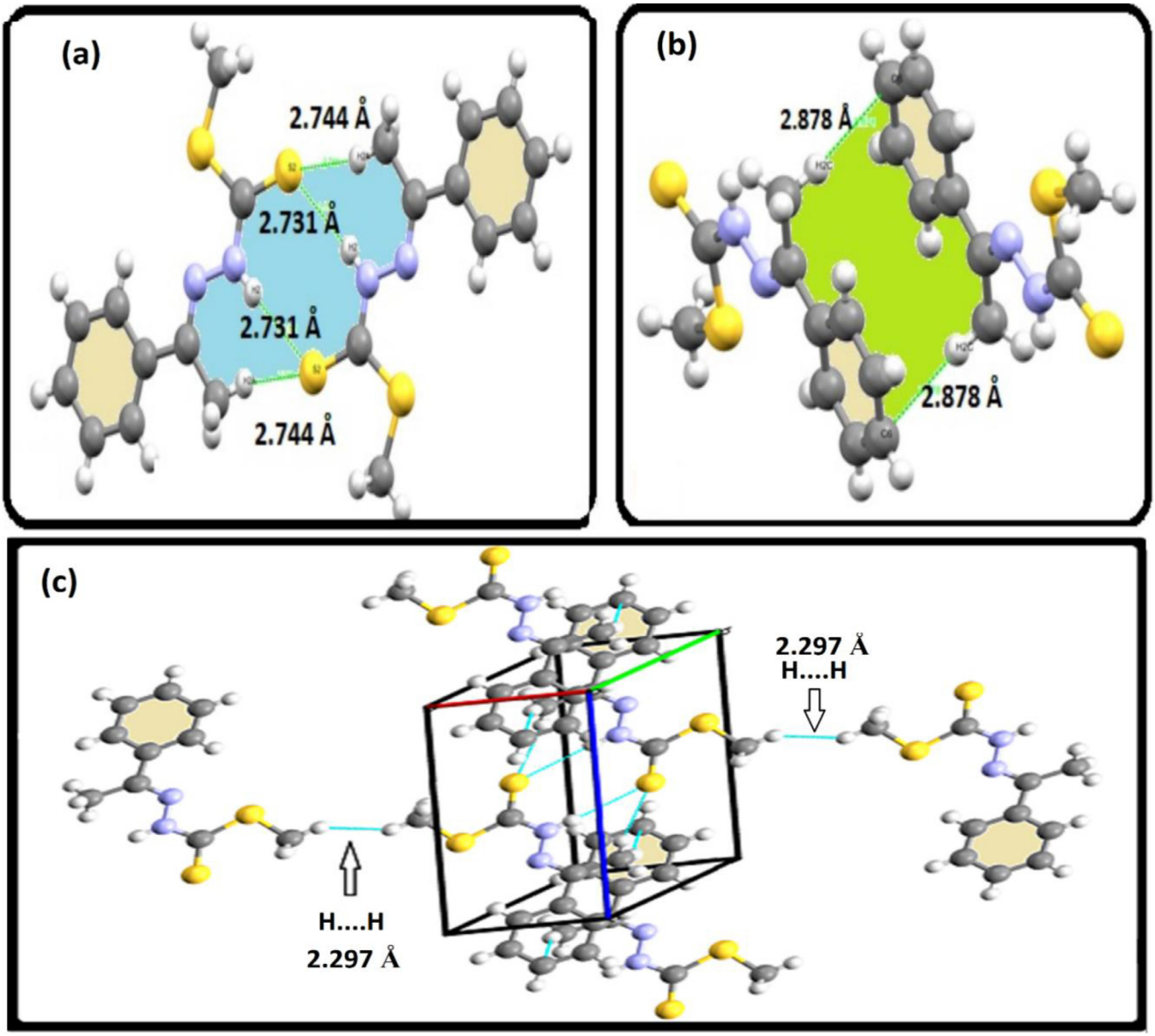

Fig. 3. Representation of all the interactions in the desired ligand lattice, (a) 2D-2S(7) synthons, (b) 2D-S(14) synthons, and (c) 1D non-polar covalent interactions.

2.4. X-ray crystallography

A colorless single-crystal suitable for XRD-measurment was collected via direct evabluration of $CHCl_3$ from diluted solution of the ligand to form block crystal with the dimension of 0.48 × 0.25 × 0.19 mm. The structure was solved using *SHELXL* and *SHELXS* programs, respectively [36].

2.4. Docking in silico studies

Docking study of (E)-methyl 2-(1-phenylethylidene) hydrazinecarbodithioate as thione and thiol isomers of the title ligand and the standard ligand, donepezil, were performed using the AutodockVina wizard in PyRx 0.8 suit based on scoring functions [37]. PyRx 0.8 suit is a known and reliable software to show the target protein and ligands innate binding conformation and protein-ligand interaction [38–40]. Settings in the program include: grid box exhaustiveness = 8, center x = 3.08836236887, center y = 61.8742805208, center z = 64.9907970034, size x = 23.3016576571, size y = 25.0, size z = 24.9905004153 for docking against 1EVE. Ligand and the standard donepezil were converted into PDB style for input to Autodock Vina in PyRx. The TcAChE (PDB: 1EVE) was saved in PDB format after deletion of the water and inhibitor molecules. The PyMOL molecular viewer was used to present the output [41]. 2-D LIGPLOT software was also used for the representation of the protein-ligand interactions [42].

3. Result and discussion

3.1. Synthesis, XRD and DFT-structure analysis

The titled compound (E)-methyl 2-(1-phenylethylidene) hydrazinecarbodithioate was prepared [15] and illustrated as in Scheme 1.

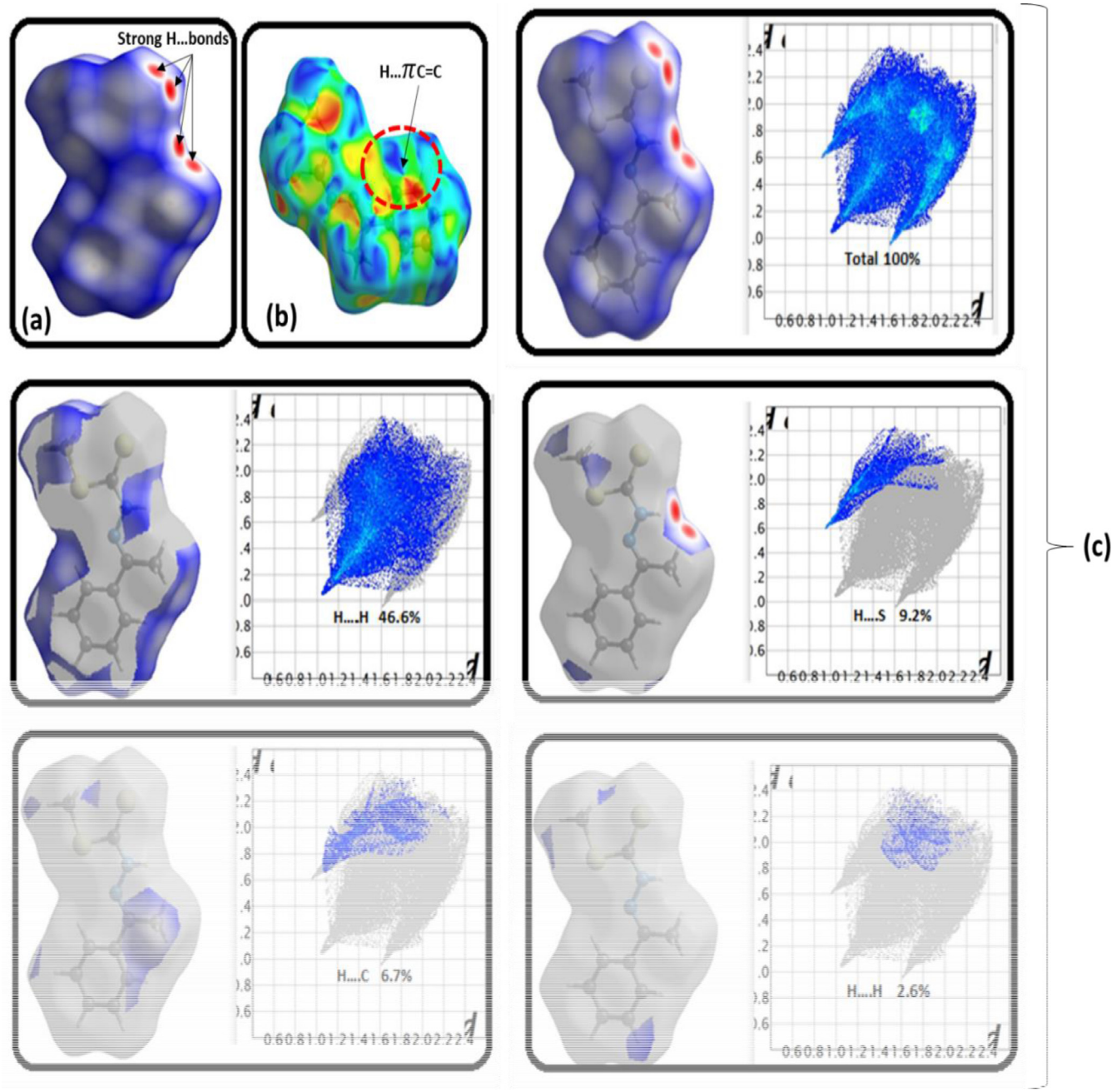

Fig. 4. (a) d_{norm} mapped, (b) Shape index and, (c) Fingerprint H…X atoms HSA calculations.

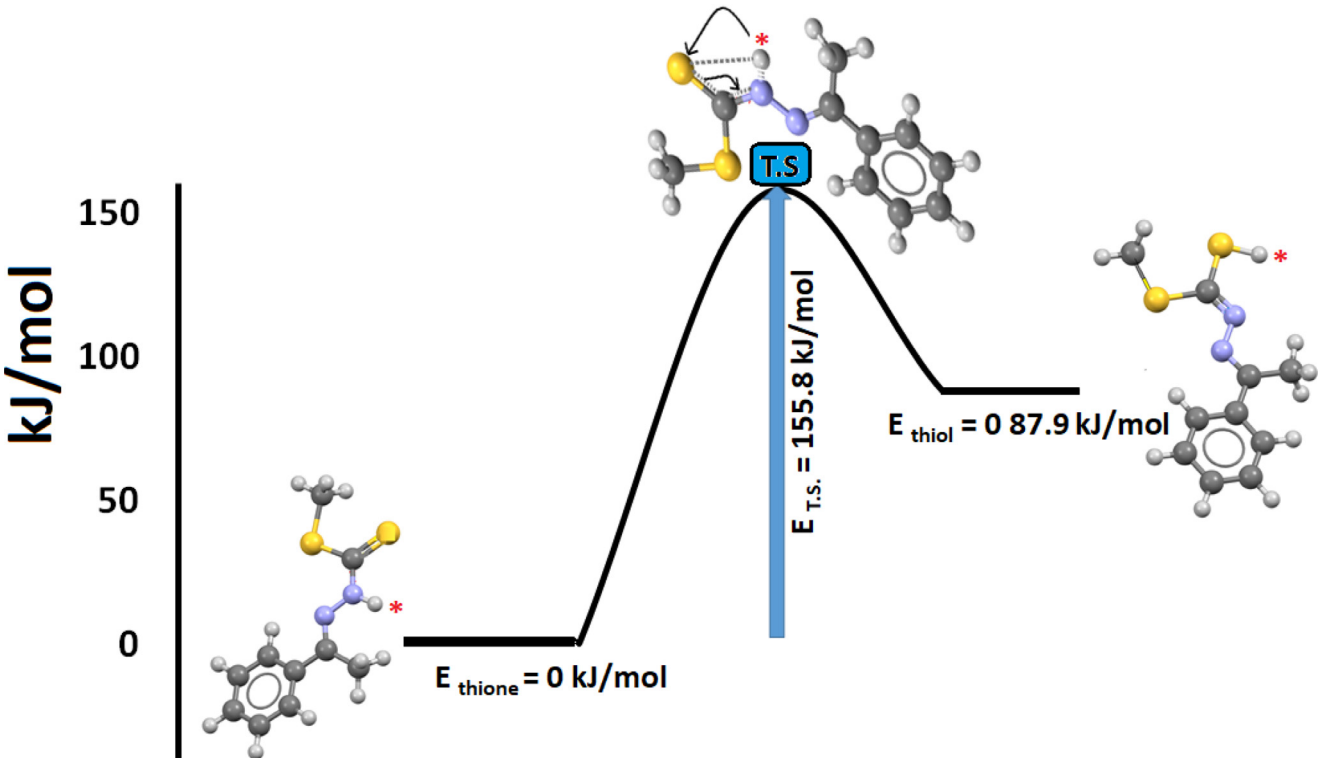

Fig. 5. The structure and energy profile of the thione<=>thiol one-step proton intra-migration.

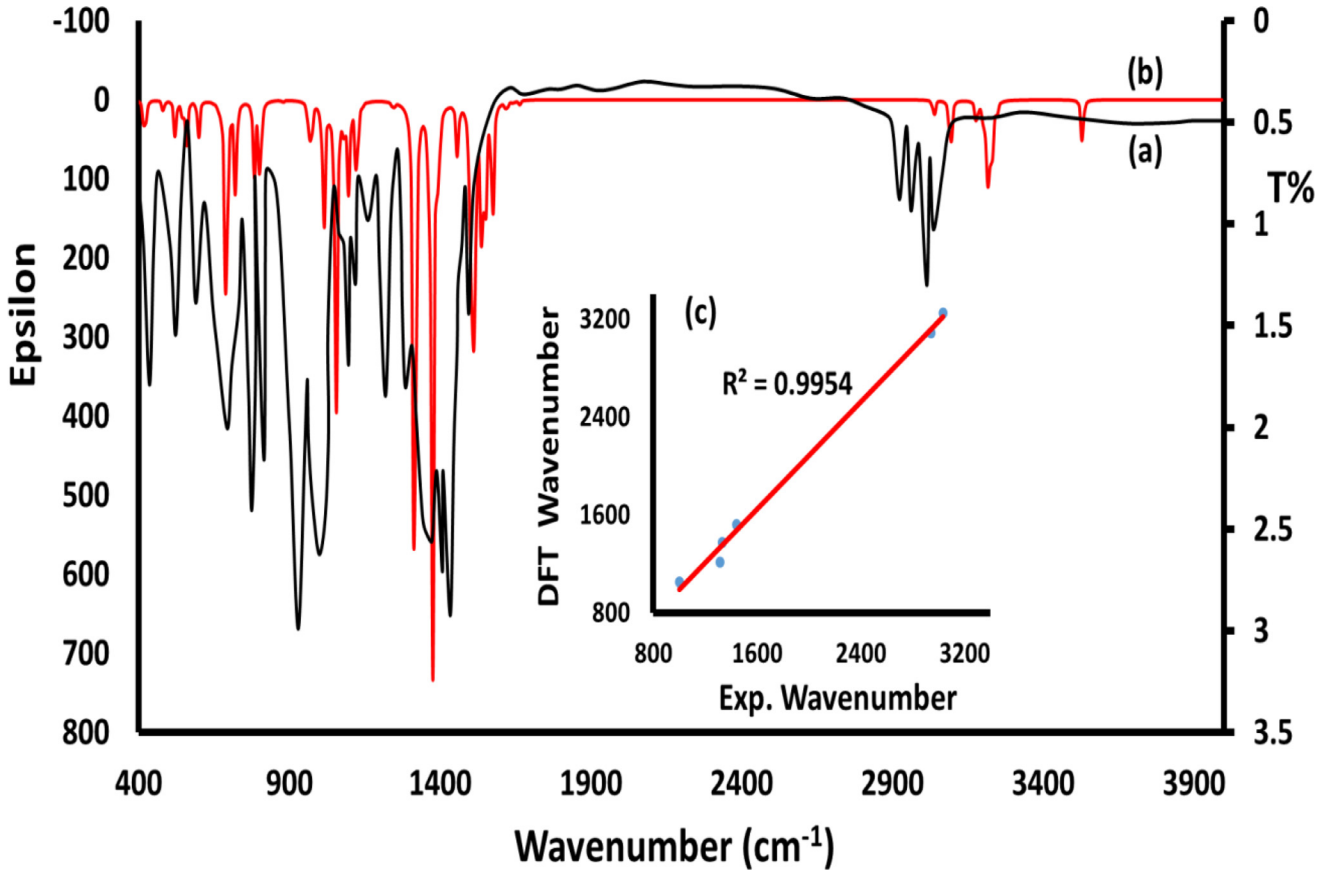

Fig. 6. FT-IR of (E)-methyl 2-(1-phenylethylidene)hydrazinecarbodithioate: (a) Exp., (b) DFT, and (c) DFT *vs.* XRD graphical relation.

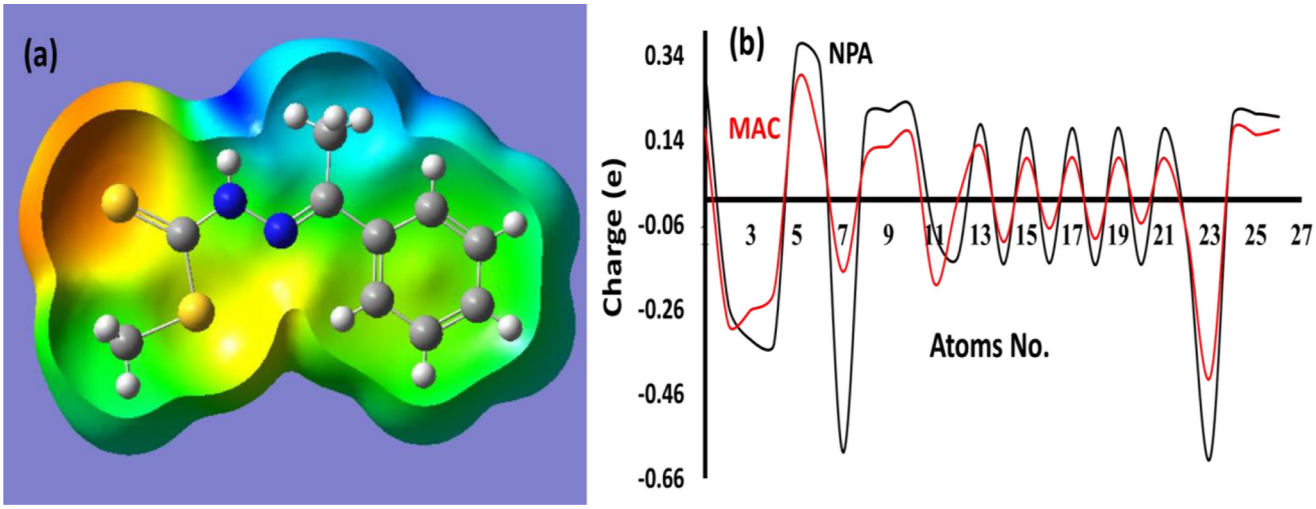

Fig. 7. (a) MEP and (b) MAC(−)/NPA(−) charge population.

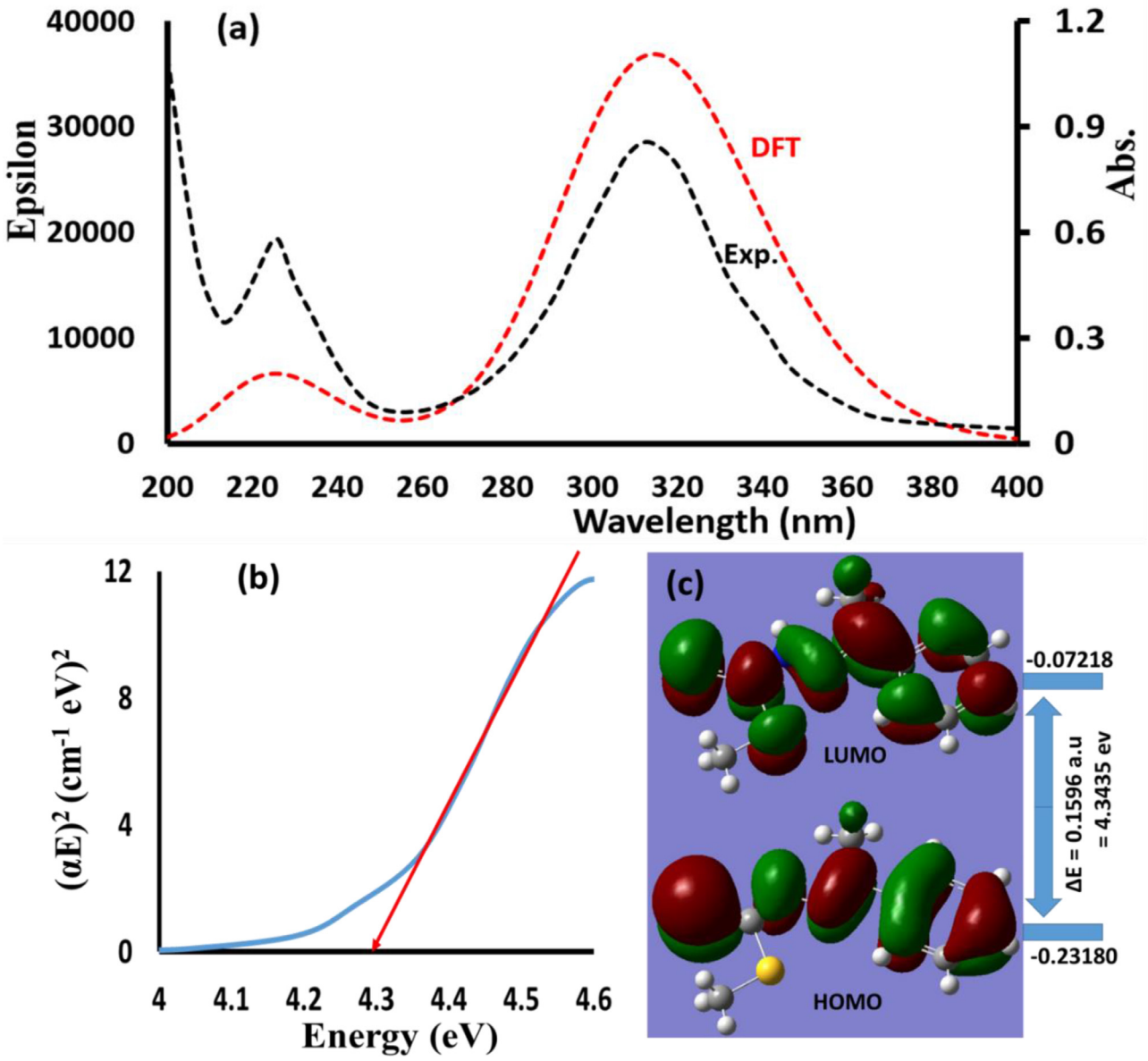

Fig. 8. (a) Abs. and TD-DFT, (b) exp. Tauc's ΔE_g and, (c) $\Delta E_{HOMO/LUMO}$ of the ligand dissolved in DMSO.

Table 1
Crystallographic refined parameters of the solved structure of desired Schiff base.

Empirical formula	$C_{10}H_{12}N_2S_2$
CCDC	1503555
Formula weight	224.34
Temperature	566(2) K
Wavelength	0.71073 Å
Crystal system	Triclinic
Space group	P-1
Unit cell dimensions	a = 5.8730(9) Å α= 82.277(3)°@@@@b = 8.2189(13) Å β= 80.044(3)°
Volume	553.24(15) $Å^3$
Z	2
Density (calculated)	1.347 mg/m^3
Absorption coefficient	0.443 mm^{-1}
F(000)	236
Crystal size	0.48 × 0.25 × 0.19 mm^3
Theta range for data collection	1.77 to 27.87°
Index ranges	-7<=h<=7, -10<=k<=10, -15<=l<=15
Reflections collected	5254
Independent reflections	2630 [R(int) = 0.0127]
Completeness to theta = 27.87°	99.5 %
Absorption correction	Semi-empirical from equivalents
Max. and min. transmission	0.9205 and 0.8155
Refinement method	Full-matrix least-squares on F^2
Data/restraints/parameters	2630/0/130
Goodness-of-fit on F^2	1.046
Final R indices [I>2sigma(I)]	R1 = 0.0384, wR2 = 0.1025
R indices (all data)	R1 = 0.0458, wR2 = 0.1086
Extinction coefficient	0.015 (4)
Largest diff. peak and hole	0.228 and -0.235 e.$Å^{-3}$

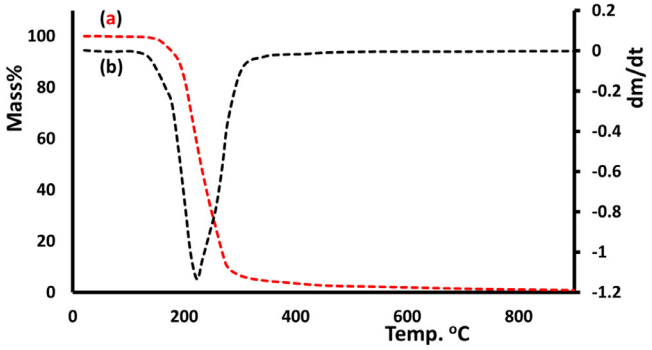

Fig. 9. TG/DTG behavior of the desired ligand.

The desired compound was crystallized in a Triclinic system with P-1 space group with Z = 2 per cell, the crytal data details were illustracted in Table 1. The compound was isolated as thioneform isomer and not thiol with N-H Schiff base ligand and *E*-isomeraround C=N bond. The S-Me, and N-N functional groups are in the same direction parallel with the phenyl group that makes the compound as planar S, N bidentate ligand as seen in Fig. 1a. The XRD-structure parameters showed all the bond lengths and angles are in their expected values and similar to the reported ones [43]. Only the S=C functional group showed longer bond length thione which supports the possibility of tautomerization process to form the thiol isomer. The B3LYP/6-311G(d,p) optimized in the gaseous phase consistent with XRD result as seen in Table 2 and Fig. 1b.

The calculated DFT and measured XRD bond distances are in an excellent agreement (Table 2 and Fig. 2a), with a correlation coefficient = 0.9931 (Fig. 2b). Similarly, XRD/DFT angles are also in good agreement as seen in Fig 2c, with a correlation coefficient = 0.9371 (Fig. 2d).

3.2. XRD/HSA-interactions

In the crystal lattice of the ligand two types of polar interactions are present: the first one formed 2D-2S(7) synthons via two C=S…H-N H-bond with 2.731 Å and the second C=S…H-C_{Me} with 2.744 Å (Fig. 3a). Fig. 3b showed the formation of 2D-S(14) synthons via two C_{Me}-H…πPh with 2.878 Å. Interestingly, one non-polar covalent interaction with two 1D H….H self-assembly

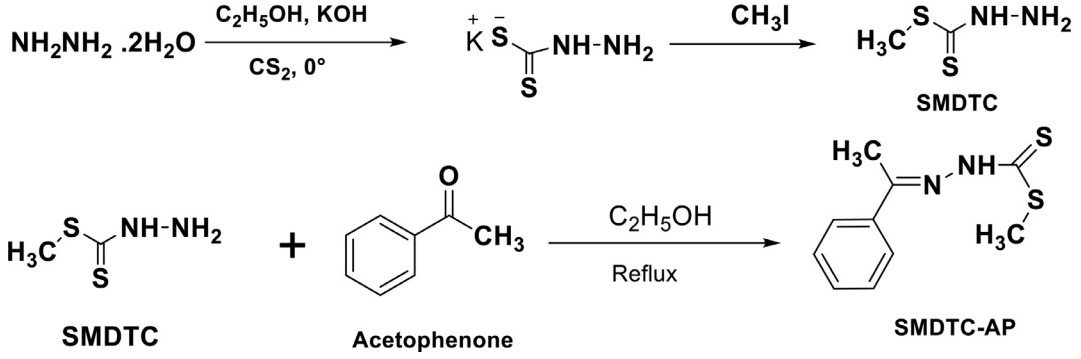

Scheme 1. Synthesis of the (E)-methyl 2-(1-phenylethylidene)hydrazinecarbodithioate.

Table 2
Experimental XRD and calculated DFT bond lengths and angles values.

Bond No.	Bonds (Å)	Exp. XRD	DFT	Angle No.	Angles (°)				Exp. XRD	DFT
1	S1	C9	1.748(2)	1.8246	1	C9	S1	C10	101.34(9)	100.44
2	S1	C10	1.797(2)	1.8844	2	N2	N1	C1	119.3(1)	119.46
3	S2	C9	1.656(2)	1.7092	3	N1	N2	C9	117.9(1)	121.8
4	N1	N2	1.377(2)	1.3768	4	N1	C1	C2	125.2(2)	122.73
5	N1	C1	1.284(2)	1.3059	5	N1	C1	C3	115.1(1)	116.23
6	N2	C9	1.347(2)	1.3631	6	C2	C1	C3	119.7(1)	121.04
7	C1	C2	1.492(3)	1.5134	7	C1	C3	C4	121.1(1)	119.97
8	C1	C3	1.486(2)	1.4816	8	C1	C3	C8	121.2(2)	121.65
9	C3	C4	1.390(2)	1.4126	9	C4	C3	C8	117.6(2)	118.38
10	C3	C8	1.385(2)	1.4088	10	C3	C4	C5	121.0(2)	120.68
11	C4	C5	1.379(3)	1.3935	11	C4	C5	C6	120.3(2)	120.4
12	C5	C6	1.378(3)	1.4021	12	C5	C6	C7	119.7(2)	119.51
13	C6	C7	1.362(3)	1.3978	13	C6	C7	C8	120.2(2)	120.27
14	C7	C8	1.389(3)	1.3986	14	C3	C8	C7	121.1(2)	120.76
					15	S1	C9	S2	125.1(1)	126.01
					16	S1	C9	N2	113.0(1)	113.53
					17	S2	C9	N2	121.9(1)	120.46

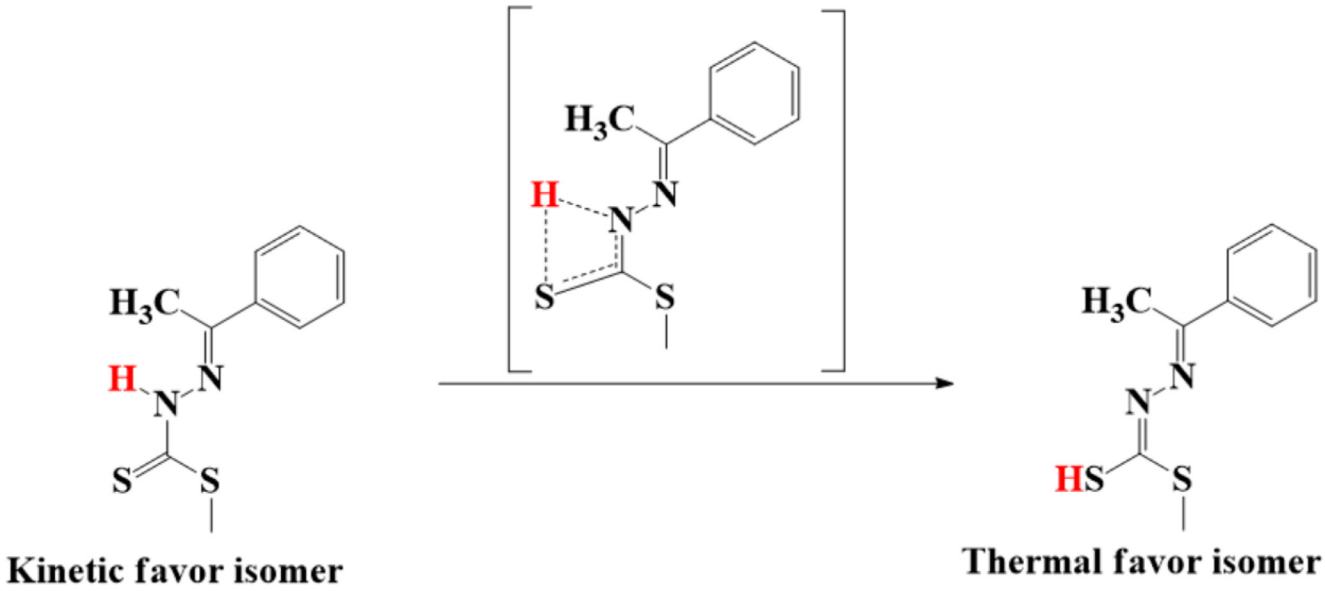

Scheme 2. Thione<=> thiol tautomerization isomerization process.

supramolecular interactions with 2.297 Å lengths were recorded as seen in Fig. 3c.

To achieve furthermore information about the interaction types in the 3D lattice HSA was carried via the crystal CIF file in the range -0.588 to 1.755 a.u [44–48]; the results were illustrated in Fig. 4. The d_{norm}-normalized reflected the presences of four big red spots due to the formation of 2N-H….S, and 2C-H…S short H-bonds that is consistent with XRD-packing H-bond formation as seen in Fig. 4a. Moreover, the formation of H…π pH interaction can be detected via the shape index model as seen in Fig. 4b. The 1D self-assembly supramolecular interaction can be conformed via the 2D-finger print plot since the H…H atoms ratios analysis reflected such interaction as a major one with 46.6% percentage as seen in Fig. 4c. Meanwhile, the rest of the other atoms interactions were calculated in the following order C••••S(9.2)>C••••H(6.7)>N••••H(2.6)>N••••H.

3.3. One-step single proton intra-migration tautomerization

Since the compound structure of the desired ligand has been solved by XRD as thione isomer, then it is a more stable isomer compared to the thiol structure. Therefore, one can consider it as kinetically favored isomer, and whereas, the thiol is the thermodynamically favored isomer as seen in Scheme 2.

As shown in Scheme 2, the desired ligand may exist only in two tautomeric thiol and thione forms. The both thione <=> thiol isomer and transition state (T.S.) geometries were optimized at the B3LYP/6-311++G(d,p) level of theory and gausses state. The DFT-computation revealed the thione tautomer the lowest energy compared to the thiol isomer which is consistent with the XRD data [20–23].

The DFT calculation supported the single H of N-H in the thione isomer transferred to the neighbor S of S=C to form thiol via intra-migration-four-membered [N-H…S=C] T.S one-step, as seen in Fig. 5. In T.S ring the S….H bond found to be longer than N….H with 1.81 and 1.45 Å, respectively. Moreover, the imaginary vibrational frequency of the detected [T.S.] in this processes is 1489i cm^{-1}, this value is consistent with the single proton intra-migration of previously recorded processes [20–23].

The gaseous minimum global energy principle profiles reflected the thiol with 87.9 kJ/mol higher than the reference thione kinetic favor isomer, meanwhile, the T.S. state is 155.8 kJ/mol higher than the thione, as seen in Fig. 5. This DFT-computation supported the theory of one-step single proton intra-migration tautomerization as well as correspond to similar scientifically reported processes [46].

Table 3
MAC and NPA charges values.

Atom No.	Atom	NPA	MAC	Atom No.	Atom	NPA	MAC
1	S	0.29965	0.165882	14	C	-0.15209	-0.10003
2	S	-0.24551	-0.29387	15	H	0.16891	0.0979
3	N	-0.3319	-0.2605	16	C	-0.14995	-0.06837
4	N	-0.33982	-0.21731	17	H	0.16914	0.099853
5	H	0.35827	0.279281	18	C	-0.15432	-0.09285
6	C	0.31348	0.141456	19	H	0.17015	0.098729
7	C	-0.59658	-0.1705	20	C	-0.15328	-0.05629
8	H	0.19435	0.099501	21	H	0.16815	0.097933
9	H	0.20924	0.12602	22	C	-0.09325	-0.08171
10	H	0.21807	0.151262	23	C	-0.61241	-0.42166
11	C	-0.07785	-0.19971	24	H	0.19657	0.16251
12	C	-0.13658	-0.00231	25	H	0.20308	0.152832
13	H	0.17826	0.127168	26	H	0.19621	0.164768

3.4. IR investigations

The solid-state experimental IR of (E)-methyl 2-(1-phenylethylidene)hydrazinecarbodithioate reflected the existence of various functional groups in the backbone of the ligand. The absence of stretching vibrations of N-H confirmed the formation of intra-hydrogen N-H…S=C bond [43]. Moreover, νC_{ph}-H was detected at ~ 3110 cm^{-1}, νC_{CH3}-H sited at 2940–2880 cm^{-1} and νC=S sited at 1030 cm^{-1} as seen in Fig. 6a.The functional groups stretching vibrations like N-N, C-O, C=C, C-N, C-C, and C-S attributed to their known vibrational positions [4–7].

In the gaseous DFT-IR stretching vibrations the N-H was detected at 3580 cm^{-1}, the νC_{ph}-H was detected at ~3280 cm^{-1}, νC_{CH3}-H sited at 3100–2820 cm^{-1} and νC=S sited at 1050 cm^{-1} as seen in Fig. 6b. Moreover, the high degree of Exp./DFT-IR compatibility was supported by the unity graphical correlation (0.998) as seen in Fig. 6c.

3.5. MEP and MAC/NPA charges

The molecular electrostatic potential (MEP) compoutions are served to get more insights of chemical reactivity of the desired molecule that related the negative with red and yellow color and positive with blue color potential sites in match with the total electron density surface of the compouted molecule. The MEP contour map of desired S.B was determined using DFT/B3LYP/6-311G(d) process. The MEP presence here of a strong nucleophilic functional groups like S=C with red color and moderate nucleophilic around the S-Me with yellow color. On an other hand, the protons of N-H, CH_3, and H-of Ph were reflected as electrophilic sites with blue color as seen in Fig. 7a. Morover, since both nucleophilic and electrophilic functional groups are recorded on the molecule surface by MEP, therefore, polar interactions (blue….red) like H….S, and H…πPh are possible to be established between molecules packed to form the lattice, such seen is agreed with XRD and HSA results [48]. To identify the charge of the atoms that composed any molecule, researchers resort to compoute the charge using DFT-theoretical method, there are many models for estimating the values of the charge for each atom, but Mulliken Atomic Charge (MAC), Natural Population Analysis (NPA) are the most famous and trusted models, the convergence in the charges calculated by MAC and NPA models increases the confidence in such calculations. MAC and NPA population charges revealed digital e-rich and e- poor, N, N, S_2=C, and all the carbons except C=S atoms are nucleophilic sites with negative charges (Table 3). On the other hand, all protons, C=S, and S_1 atoms are electrophilic sites with positive charge as in Fig. 7b. Herein, it can be seen that MEP and MAC/NPA plays an important role in estimating the charge of the atoms, especially the outer atoms constituents of the surface of the compound, therefore, the binding behavior of the compound with its neighbor to build the crystal lattice can be established. The NPA and MAC result in this study matched well with the MEP and HSA/XRD-packing result.

3.6. Absorbance/TD-SCF-B3LYP and ΔEg/HOMO-LUMO

UV–Vis absorption spectrum of the (E)-methyl 2-(1-phenylethylidene)hydrazinecarbodithioate dissolved in DMSO in region 200–800 nm was determined as seen in Fig. 8a. Two absorption bands centered at λ_{max}= 225 and λ_{max}= 312 nm with ε = 2605 and 3820, $Lmol^{-1}cm$-1, have been recorded respectively. These UV-peaks can be assigned to $\pi \rightarrow \pi^*$ and n→π^* electron transition, respectively. No other bands in the visible area were detected. Time-dependent DFT/B3LYP computation has been carried out to understand the theoretical UV–Vis electronic transitions using the same solvent, and then compare it with the experimental result. The calculated wavelength (nm) and oscillator strength (f) with the aid of the method are summarized in Table 4. The experimental peaks of the desired ligand have been matched by means of TD-DFT calculations as seen in Fig. 8b. The experimental band at λ_{max}= 225 nm ($\pi \rightarrow \pi^*$) matched well to the TD-DFT band observed at 226.8 nm ($\Delta\lambda$ =1.8 nm) can be dominated by the HOMO-4→LUMO(30%), HOMO-2→L+1(28%), HOMO-1→LUMO+2(24%) major contributions and HOMO-3→LUMO(4%), HOMO-3→LUMO+1 (2%), HOMO-1→LUMO+1(4%), HOMO→LUMO+5 (3%) as minor contributions electron transfer. The experimental peak at λ_{max}= 312 nm (n→π^*) was matched well to TD-DFT band at 315.1 nm ($\Delta\lambda$ =3.1 nm) whereas corresponded to HOMO+1→LUMO (97%) as major contributions and HOMO-2→LUMO+2 (3%) as minor contributions electron transfer.

The Tauc ΔE_g [49] direct experimental optical band gap energy was recorded in DMSO, the measured ΔE_g found to 4.30 eV as seen in Fig. 6c, this result isapproximated with the HOMO→LUMO theoretical electron transfer energy, $\Delta E_{HOMO/LUMO}$= 4.34 eV as can be seen in Fig. 8c.

3.7. Thermal behavior

The TG/DTG-curves of Methyl-(E)-2-(phenylmethylidene) dithiocarbazatewereperformed in a temperature range of 20 to 900 °C under 5 °C/minute heating rate and open O_2-atmosphere, the result is shown in Fig. 9a. The ligand showed a high degree of thermal stability, it was stable up to 198 °C. Above this temperature, the ligand decayed from 99% to ~1 mass% up to 300 °C in a broad one-step decomposition process with TDTG = 218 °C as in Fig. 9b.

Table 4
TD-DFT electron transfer detail data of the desired ligand dissolved in DMSO.

No.	λ (nm)	Osc. Str. (f)	Major contributions	Minor contributions
1	366.58	0.001	HOMO->LUMO(91%)	HOMO->L+1(7%)
2	315.10	0.712	H-1->LUMO(97%)	H-2->L+2(3%)
3	290.09	0.095	H-2->LUMO(96%)	H-1->L+2(4%)
4	263.86	0.019	H-3->LUMO(74%), H-1->L+2(11%)	HOMO->L+1(7%)
5	263.49	0.002	HOMO->L+1(82%)	H-3->LUMO(6%), HOMO->LUMO(7%)
6	250.13	0.001	H-5->LUMO(97%)	–
7	242.07	0.029	H-4->LUMO(25%), H-1->L+1(69%)	–
8	231.10	0.044	H-4->LUMO(20%), H-3->LUMO(10%), H-1->L+2(50%)	H-3->L+1(2%), H-2->L+1(5%), H-1->L+1(8%)
9	226.81	0.200	H-4->LUMO (30%), H-2->L+1 (28%), H-1->L+2 (24%)	H-3->LUMO(4%), H-3->L+1(2%), H-1->L+1(4%), HOMO->L+5(3%)
10	212.70	0.014	H-3->L+1 (19%), H-2->L+2 (69%)	H-4->LUMO 2%), H-3->LUMO(3%)

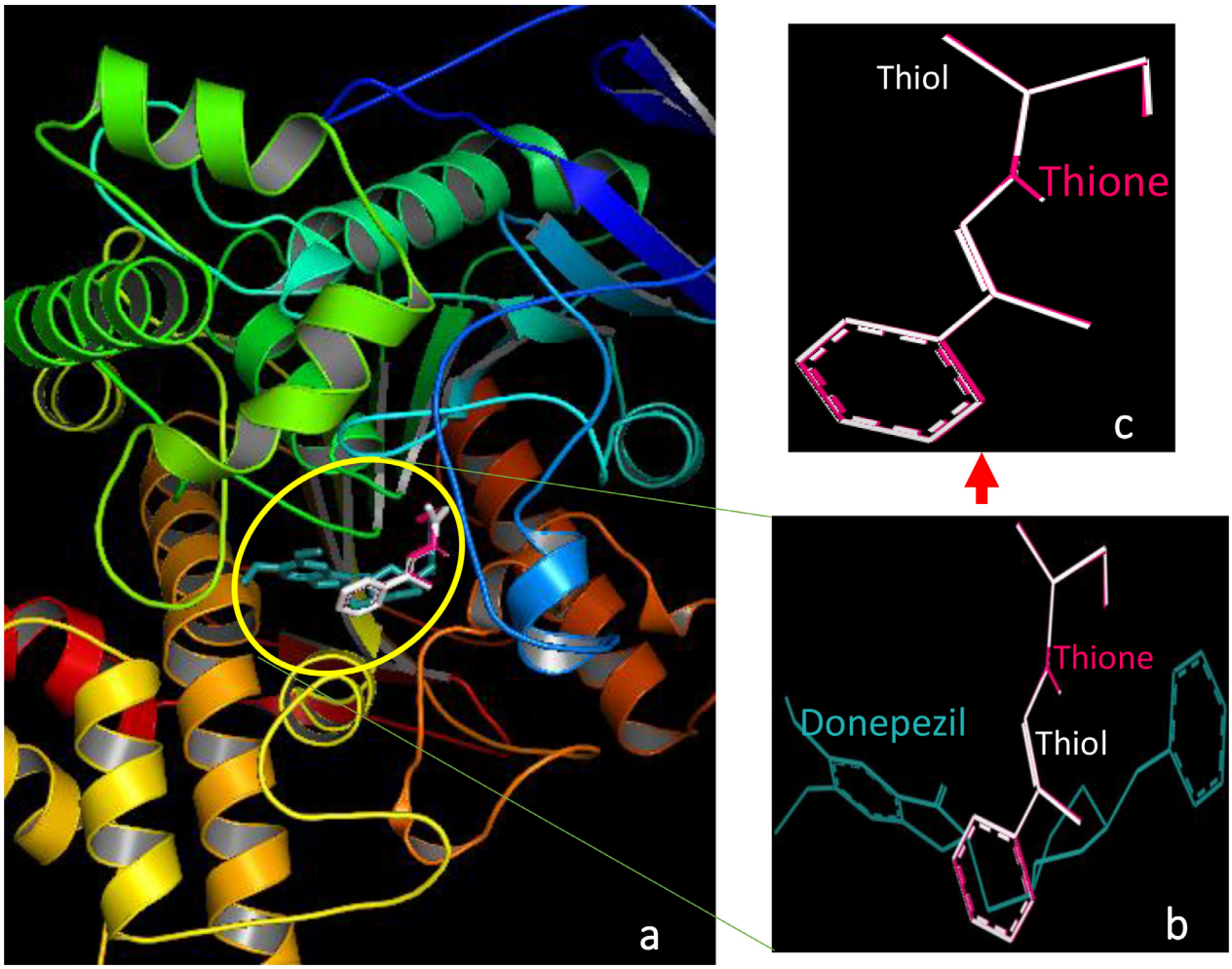

Fig. 10. (a) The superposition of the desired ligand (thione-magenta and thiol-white isomers) and donepezil-deepteal sticks [50] docked under identical conditions; (b) The superposition of donepezil and the title ligand (thione and thiol) without the 1EVE protease for clarity, and (c) Thethione and thiol isomers in the active sites of the AChE.

3.8. Docking analysis

The aim of this docking study is to inspect how the prepared ligand, in its different forms; thione and thiol, might bind with the active site of the TcAChE enzyme (PDB, 1EVE) as possible selective acetylcholinesterase inhibitors. The docked ligand of (E)-methyl 2-(1-phenylethylidene)-hydrazinecarbodithioatehas interacted with the active site of 1EVE as shown in Fig. 10. Noticeably, the docking results revealed that the thione isomer has overlapped most of thiol isomer indicating an obvious similarity in the interaction behavior between the thione and thiols isomers against 1EVE Fig. 10(c). The title ligand appeared perpendicular to the standard donepezil, in the active site of the TcAChE enzyme. The binding affinity against the Torpedo California acetylcholinesterase (TcAChE), (PDB, 1EVE) is related to the number of hydrogen bonding and hydrophobic interactions. Interestingly, the title liganddisplayed good binding affinity against the TcAChE enzyme with docking score, -7.2, -7.2 kcal/mol for thione and thiol respectively in comparison to our standard compound, donepezil (-11.2 kcal/mol) docked under identical conditions.

Superimposition of our ligand and donepezil are presented in Fig. 10 demonstrating the structure of the protein–drug complex framework within the active site of 1EVE. The interactions of the prepared ligand and donepezil against the active site of AChE (1EVE) are well presented by the intensive hydrophobic interactions between the ligand and the active amino acid residues of the

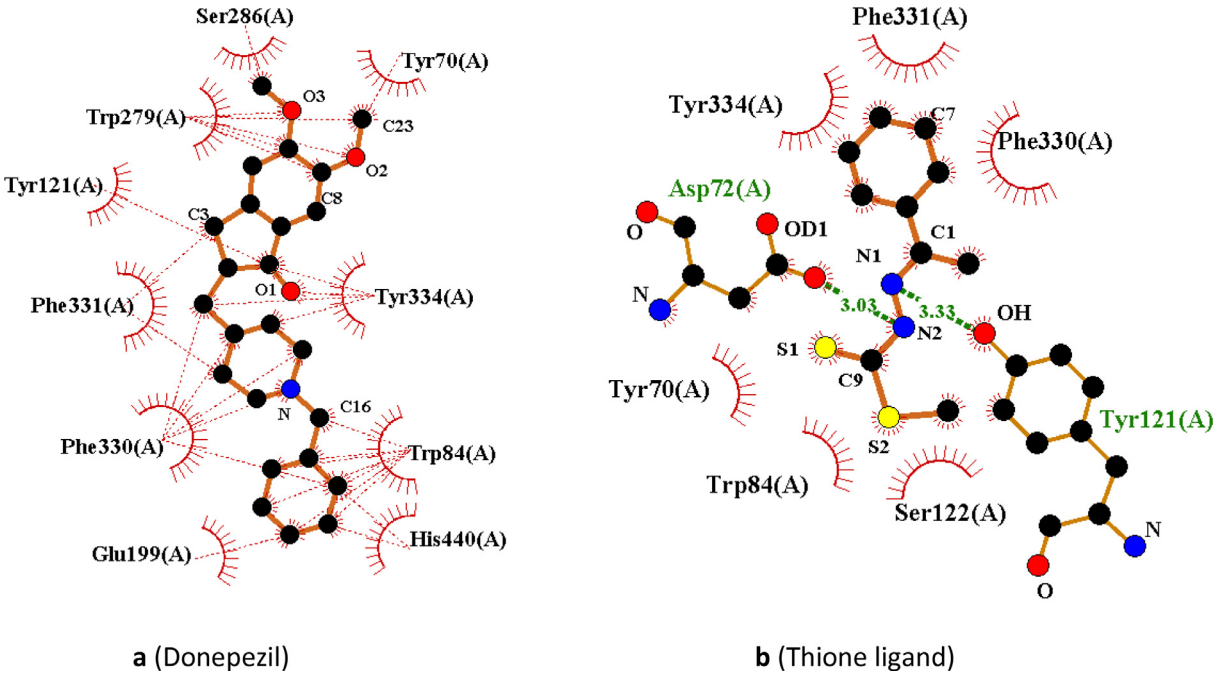

Fig. 11. (a) A schematic 2-D LIGPLOT representation of 1EVE against donepezil (brown sticks) showing hydrophobic interactions and (b) A schematic 2-D LIGPLOT representation of 1EVE against the ligand (brown sticks) showing H-bonds and hydrophobic interactions (red dashed lines are omitted for clarity) [42].

receptor, mainly via the $\pi \bullet\bullet\bullet \pi$ stacking and the lone pair of electrons on the S, O and N atoms in Fig. 11. Unexpectedly, the interaction of donepezil against AChE (1EVE) shows no H-bonds, whereas, two hydrogen bonds were observed between the title ligand and Asp-72 (3.03 A°) and Tyr-121 (3.33 A°). It is observed here as it has been well documented that the active amino acid residue (Trp84) of the receptor was considered as the main component of the anionic site [51]. It is also worth noting that at the bottom of the gorge, $\pi - \pi$ hydrophobic interaction was seen between one ring of donepezil and the phenyl moiety of His440, the active amino acid residues of the catalytic triad in the active site of AChE [52], which is completely absent in the case of our ligand against AChE (1EVE). These interactions observed in donepezil might be, in part, responsible for the low binding energy to the enzyme hence improves the inhibition effect. Importantly, the low docking score of our ligand (-7.2 kcal/mol) and the many common interaction residues found between our ligand against AChE (1EVE), from one side, and the standard donepezil against AChE (1EVE), on the other side (PHE331, TYR334, PHE330, TRP84, TYR70, and TYR121, Fig. 11), might suggest that our ligand may serve as a potential drug for treating AD.

4. Conclusion

(E)-methyl 2-(1-phenylethylidene)hydrazinecarbodithioate as thione simple-model kinetically favored structure has been proved by the XRD-crystal structure. The DFT optimized structure and structural parameters agreed well with their XRD-structure relatives. Moreover, HSA/MEP/MAC/NPC charge density quantum parameters clarified the presence of H.....S and H....π-pH interactions agreeing with the XRD-packing result. QST2/DFT method succeeded to explain the thione$\Leftrightarrow$thiol single proton tautomerization process. The TD-SCF/DFT and HOMO/LUMO energy level calculations correlated to an excellent degree with experimental electron transfer and Tauc's energy ΔE_g, respectively.The compound as most of the organic material decomposed in one-step mechanism but with a significant degree of thermal stability. The two identified isomers of our ligand showed a closer feature to the standard donepezil drug used in this study creating hope to be a possible selective acetylcholinesterase inhibitor.

Authorship statement

All persons who meet authorship criteria are listed as authors, and all authors certify that they have participated sufficiently in the work to take public responsibility for the content, including participation in the concept, design, analysis, writing, or revision of the manuscript.

Declaration of Competing Interest

There are no conflicts to declare.

Acknowledgements

The authors extend their sincere thanks to Dr. Ulrich Flörke Department Chemie, Universität Paderborn, WarburgerStrasse 100, 33098 Paderborn, Germany for solvingthe crystal structures of the Schiff bases. Similar thanks go to the staff member at Chemistry department, Faculty of Science, Benghazi University; Miss Huda MuftahSheppaek, Miss Wjdan Omar Algezzeri, and Mrs. Eman Mahmoud for their help to prepare the Schiff base, and special thanks goes to Mr. Gian L Gatti the CEO of SPCG (Swiss Petro Chemical Group) SA, Switzerland, for their support, and help.Another special thanks go to Manchester salt and Catalysis Ltd, UK and Express Cargo UK Ltd.

References

[1] M.H. Torre, D. Gambino, J. Araujo, H. Cerecetto, M. González, M.L. Lavaggi, A. Azqueta, A. López De Cerain, A.M. Vega, U. Abram, A.J. Costa-Filho, Novel Cu(II) quinoxaline N1,N4-dioxide complexes as selective hypoxic cytotoxins, Eur. J. Med. Chem. 40 (2005) 473–480, doi:10.1016/j.ejmech.2004.11.012.
[2] D.R. Richardson, P.V. Bernhardt, Crystal and molecular structure of 2-hydroxy-1-naphthaldehyde isonicotinoyl hydrazone (NIH) and its iron(III) complex: an iron chelator with anti-tumour activity, J. Biol. Inorg. Chem. 4 (1999) 266–273, doi:10.1007/s007750050312.

[3] P.B.A. Santra, P. Brandao, G. Mondal, P. Bera, A. Jana, I. Bhattacharyya, C. Pramanik, A. Santra, P. Brandao, G. Mondal, P. Bera, A. Jana, I. Bhattacharyya, C. Pramanik, P. Bera, Inorg. Chim. Acta 501 (2020) 119315.

[4] M.X. Li, L.Z. Zhang, C.L. Chen, J.Y. Niu, B.S. Ji, Synthesis, crystal structures, and biological evaluation of Cu(II) and Zn(II) complexes of 2-benzoylpyridine Schiff bases derived from S-methyl- and S-phenyldithiocarbazates, J. Inorg. Biochem. 106 (2012) 117–125, doi:10.1016/j.jinorgbio.2011.09.034.

[5] M.T. Basha, J.D. Chartres, N. Pantarat, M. Akbar Ali, A.H. Mirza, D.S. Kalinowski, D.R. Richardson, P.V. Bernhardt, Heterocyclic dithiocarbazate iron chelators: Fe coordination chemistry and biological activity, Dalt. Trans. 41 (2012) 6536–6548, doi:10.1039/c2dt12387h.

[6] P.I.d.S. Maia, A.G.d.A. Fernandes, J.J.N. Silva, A.D. Andricopulo, S.S. Lemos, E.S. Lang, U. Abram, V.M. Deflon, Dithiocarbazate complexes with the [M(PPh_3)]2+ (M=Pd or Pt) moiety. Synthesis, characterization and anti-Tripanosoma cruzi activity, J. Inorg. Biochem. 104 (2010) 1276–1282, doi:10.1016/j.jinorgbio.2010.08.009.

[7] P.K. Sasmal, A.K. Patra, A.R. Chakravarty, Synthesis, structure, DNA binding and DNA cleavage activity of oxovanadium(IV) N-salicylidene-S-methyldithiocarbazate complexes of phenanthroline bases, J. Inorg. Biochem. 102 (2008) 1463–1472, doi:10.1016/j.jinorgbio.2007.12.031.

[8] Y.T. Liu, G.D. Lian, D.W. Yin, B.J. Su, Synthesis, characterization and biological activity of ferrocene-based Schiff base ligands and their metal (II) complexes, in: Spectrochim. Acta - Part A Mol. Biomol. Spectrosc., Elsevier, 2013, pp. 131–137, doi:10.1016/j.saa.2012.03.049.

[9] L.Z. Zhang, T. Ding, C.L. Chen, M.X. Li, D. Zhang, J.Y. Niu, Biological activities of pyridine-2-carbaldehyde Schiff bases derived from S-methyl- and S-benzyldithiocarbazate and their zinc(II) and manganese(II) complexes. Crystal Structure of the Manganese(II) complex of pyridine-2-carbaldehyde S-benzyldithiocarbazate, Russ. J. Coord. Chem. Khimiya. 37 (2011) 356–361, doi:10.1134/S1070328411040117.

[10] T.Khatib N.Al-Zaqri, A. Alsalme, F.A. Alharthi, A. Zarrouk, I. Warad, Synthesis and amide imidic prototropic tautomerization in thiophene-2-carbohydrazide: XRD, DFT/HSA-computation, DNA-docking, TG and isoconversional kinetics via FWO and KAS models, R RSC Adv. 10 (2020) 2037, doi:10.1039/c9ra09831c.

[11] A.G. Blanco, M. Sola, F.X. Gomis-Rüth, M. Coll, Tandem DNA Recognition by PhoB, a two-component signal transduction transcriptional activator, Structure 10 (2002) 701–713, doi:10.1016/S0969-2126(02)00761-X.

[12] T. Fukushima, M. Takata, C. Morrison, R. Araki, A. Fujimori, M. Abe, K. Tatsumi, M. Jasin, P.K. Dhar, E. Sonoda, T. Chiba, S. Takeda, Genetic analysis of the DNA-dependent protein kinase reveals an inhibitory role of Ku in late S-G2 phase DNA double-strand break repair, J. Biol. Chem. 276 (2001) 44413–44418, doi:10.1074/jbc.M106295200.

[13] M.T.H. Tarafder, M.T. Islam, M.A.A.A.A. Islam, S. Chantrapromma, H.K. Fun, Bis[benzyl N′-(3-phenylprop-2-enylidene)hydrazinecarbodithioato- κ2 N′,S]copper(II), Acta Crystallogr. Sect. E Struct. Reports Online. 64 (2008) m416–m417, doi:10.1107/S1600536808002262.

[14] M.A. Ali, H.J. Hj Abu Bakar, A.H. Mirza, S.J. Smith, L.R. Gahan, P.V. Bernhardt, Preparation, spectroscopic characterization and X-ray crystal and molecular structures of nickel(II), copper(II) and zinc(II) complexes of the Schiff base formed from isatin and S-methyldithiocarbazate (Hisa-sme), Polyhedron 27 (2008) 71–79, doi:10.1016/j.poly.2007.08.022.

[15] M. Akbar Ali, M.T.H. Tarafdar, Metal complexes of sulphur and nitrogen-containing ligands: complexes of s-benzyldithiocarbazate and a schiff base formed by its condensation with pyridine-2-carboxaldehyde, J. Inorg. Nucl. Chem. 39 (1977) 1785–1791, doi:10.1016/0022-1902(77)80202-9.

[16] M.E. Hossain, M.N. Alam, J. Begum, M. Akbar Ali, M. Nazimuddin, F.E. Smith, R.C. Hynes, The preparation, characterization, crystal structure and biological activities of some copper(II) complexes of the 2-benzoylpyridine Schiff bases of S-methyl- and S-benzyldithiocarbazate, Inorganica Chim. Acta 249 (1996) 207–213, doi:10.1016/0020-1693(96)05098-0.

[17] A.M. Boshaala, A. Alfarhan, H. Muftah, W. Omar, Crystal interaction, XRD powder, and Hirshfeld surface analysis of S- benzyl- β -N- (1- (4-chlorophenyl) ethylidene) dithiocarbazate Schiff base, Mor. J. Chem. 4 (2020) 1048–1055.

[18] A.M. Boshaala, K. Alfarhan, H. Muftah, W. Omar, A. Zarrouk, I. Warad, Crystal interaction, XRD powder, and Hirshfeld surface analysis of S- benzyl- β -N-(1- (4-chlorophenyl) ethylidene) dithiocarbazate Schiff base, Mor. J. Chem. 4 (2020) 1048–1055.

[19] Y.Q. Ding, Y.Z. Cui, T.D. Li, New views on the reaction of primary amine and aldehyde from DFT study, J. Phys. Chem. A. 119 (2015) 4252–4260, doi:10.1021/acs.jpca.5b02186.

[20] V. Arjunan, R. Santhanam, T. Rani, H. Rosi, S. Mohan, Conformational, vibrational, NMR and DFT studies of N-methylacetanilide, Spectrochim. Acta - Part A Mol. Biomol. Spectrosc. 104 (2013) 182–196, doi:10.1016/j.saa.2012.11.037.

[21] S. Sevvanthi, S. Muthu, M. Raja, Molecular docking, vibrational spectroscopy studies of (RS)-2-(tert-butylamino)-1-(3-chlorophenyl)propan-1-one: A potential adrenaline uptake inhibitor, J. Mol. Struct. 1173 (2018) 251–260, doi:10.1016/j.molstruc.2018.07.001.

[22] A. Barakat, M.S. Islam, A.M. Al-Majid, H.A. Ghabbour, S. Atef, A. Zarrouk, I. Warad, Quantum chemical insight into the molecular structure of L-chemosensor 1,3-dimethyl-5-(thien-2-ylmethylene)-pyrimidine-2,4,6-(1 H,3 H,5 H)-trione: naked-eye colorimetric detection of copper(II) anions, J. Theor. Comput. Chem. 17 (2018) 1–23, doi:10.1142/S0219633618500050.

[23] A. Barakat, S.M. Soliman, H.A. Ghabbour, M. Ali, A.M. Al-Majid, A. Zarrouk, I. Warad, Intermolecular interactions in crystal structure, Hirshfeld surface, characterization, DFT and thermal analysis of 5-((5-bromo-1H-indol-3-yl)methylene)-1,3-dimethylpyrimidine-2,4,6(1H,3H,5H)-trione indole, J. Mol. Struct. 1137 (2017) 354–361, doi:10.1016/j.molstruc.2017.02.041.

[24] Y. Zi, M. Zhu, X. Li, Y. Xu, H. Wei, D. Li, C. Mu, Effects of carboxyl and aldehyde groups on the antibacterial activity of oxidized amylose, Carbohydr. Polym. 192 (2018) 118–125, doi:10.1016/j.carbpol.2018.03.060.

[25] J.E. Barnsley, P. Wagner, D.L. Officer, K.C. Gordon, Aldehyde isomers of porphyrin: a spectroscopic and computational study, J. Mol. Struct. 1173 (2018) 665–670, doi:10.1016/j.molstruc.2018.06.117.

[26] Y. Meng, X. Zhang, M. Mezei, M. Cui, Molecular docking: a powerful approach for structure-based drug discovery. Current computer-aided drug design, Curr. Comput. Aided Drug Des. 7 (2011) 146–157.

[27] I. Guedes, C. de Magalhães, L.D.-B. Reviews, U. 2014, Receptor–ligand molecular docking, Biophys. Rev. 6 (2014) 75–87.

[28] P.L.H., D.P. Arya, Natural product DNA major groove binders, Nat. Prod. Rep. 29 (2012) 134–143.

[29] S.U. Rehman, T. Sarwar, M.A. Husain, H.M. Ishqi, M. Tabish, Studying non-covalent drug-DNA interactions, Arch. Biochem. Biophys. 576 (2015) 49–60, doi:10.1016/j.abb.2015.03.024.

[30] F. Arjmand, S. Parveen, M. Afzal, M. Shahid, Synthesis, characterization, biological studies (DNA binding, cleavage, antibacterial and topoisomerase I) and molecular docking of copper(II) benzimidazole complexes, J. Photochem. Photobiol. B Biol. 114 (2012) 15–26, doi:10.1016/j.jphotobiol.2012.05.003.

[31] E. Bonandi, M.S. Christodoulou, G. Fumagalli, D. Perdicchia, G. Rastelli, D. Passarella, The 1, 2, 3-triazole ring as a bioisostere in medicinal chemistry, Drug Discov. Today. 22 (2017) 1572–1581, doi:10.1016/j.drudis.2017.05.014.

[32] M. Weinstock, Selectivity of cholinesterase inhibition, CNS Drugs 12 (1999) 307–323, doi:10.2165/00023210-199912040-00005.

[33] J.K. Dhanjal, S. Sharma, A. Grover, A. Das, Use of ligand-based pharmacophore modeling and docking approach to find novel acetylcholinesterase inhibitors for treating Alzheimer's, Biomed. Pharmacother. 71 (2015) 146–152, doi:10.1016/j.biopha.2015.02.010.

[34] M.A.S.S.K. Wolff, D.J. Grimwood, J.J. Mckinnon, D. Jayatilaka, Crystal Explorer 3.0, University of Western Australia, Perth, Western Australia, 2007.

[35] W.C.M.J. Frisch, G.W. Trucks, H.B. Schlegel, G.E. Scuseria, M.A. Robb, J.R. Cheeseman, G. Scalmani, V. Barone, B. Mennucci, G.A. Petersson, H. Nakatsuji, Gaussian 09, Gaussian Inc., Wallingford CT, 2009.

[36] G.M. Sheldrick, A short history of SHELX, Acta Crystallogr. Sect. A Found. Crystallogr. 64 (2008) 112–122, doi:10.1107/S0108767307043930.

[37] A. Allouche, Software news and updates gabedit-a graphical user interface for computational chemistry softwares, J. Comput. Chem. 32 (2012) 174–182, doi:10.1002/jcc.

[38] D.X. Liu, J.Q. Liang, T.S. Fung, in: Human Coronavirus-229E, -OC43, -NL63, and -HKU1, Life Sci., Elsevier, 2020, pp. 1–13, doi:10.1016/b978-0-12-809633-8.21501-x.

[39] S. Luo, G.B. Lenon, H. Gill, A. Hung, D.A. Dias, M. Li, L.T. Nguyen, Inhibitory effect of a weight-loss Chinese herbal formula RCM-107 on pancreatic α-amylase activity: Enzymatic and in silico approaches, PLoS One 15 (2020) 1–17, doi:10.1371/journal.pone.0231815.

[40] J. Duncan, Participation in global governance: coordinating "the voices of those most affected by food insecurity", Glob. Food Secur. Gov. 1263 (2015) 1–11, doi:10.1007/978-1-4939-2269-7.

[41] W.L. DeLano, PyMOL Reference Guide, Delano Sci. San Carlos, CA, US, 2004.

[42] A.C. Wallace, R.A. Laskowski, J.M. Thornton, Ligplot: a program to generate schematic diagrams of protein-ligand interactions, Protein Eng. Des. Sel. 8 (1995) 127–134, doi:10.1093/protein/8.2.127.

[43] A. Boshaala, U. Flörke, B.M. Yamin, Y.O.B. Amer, G.S.H. Ghaith, A.A. Almughery, A. Zarrouk, I. Warad, Crystal interaction, Hirshfeld surface analysis, and spectral analysis of new Dithiocarbazate Schiff bases derivative (LH) and its neutral cis-Cu(L)2 complex, J. Mol. Struct. 1224 (2021) 129207, doi:10.1016/j.molstruc.2020.129207.

[44] A. Titi, T. Shiga, H. Oshio, R. Touzani, B. Hammouti, M. Mouslim, I. Warad, Synthesis of novel Cl2Co4L6 clusterusing 1-hydroxymethyl-3,5-dimethylpyrazole (LH) ligand: crystal structure, spectral, thermal, Hirschfeld surface analysis and catalytic oxidation evaluation, J. Mol. Struct. (2020) 1199, doi:10.1016/j.molstruc.2019.126995.

[45] I. Warad, F.F. Awwadi, B. Abd Al-Ghani, A. Sawafta, N. Shivalingegowda, N.K. Lokanath, M.S. Mubarak, T. Ben Hadda, A. Zarrouk, F. Al-Rimawi, A.B. Odeh, S.A. Barghouthi, A. Al-Ghani, A. Sawafta, N. Shivalingegowda, K. Lokanath, M.S. Mubarak, T. Ben Hadda, A. Zarrouk, F. Al-Rimawi, A.B. Odeh, S.A. Barghouthi, Ultrasound-assisted synthesis of two novel [CuBr(diamine) 2.H_2O]Br complexes: Solvatochromism, crystal structure, physicochemical, Hirshfeld surface thermal, DNA/binding, antitumor and antibacterial activities, Ultrason. Sonochem. 48 (2018) 1–10, doi:10.1016/j.ultsonch.2018.05.009.

[46] I. Warad, S. Musameh, A. Sawafta, P. Brandão, C. José Tavares, A. Zarrouk, S. Amereih, A. Al Ali, R. Shariah, Ultrasonic synthesis of Oct. trans-Br2Cu(N ∩ N)2 Jahn-Teller distortion complex: XRD-properties, solvatochromism, thermal, kinetic and DNA-binding evaluations, Ultrason. Sonochem. 52 (2019) 428–436, doi:10.1016/j.ultsonch.2018.12.019.

[47] F.A. Saleemh, S. Musameh, A. Sawafta, P. Brandao, C.J. Tavares, S. Ferdov, A. Barakat, A. Al Ali, M. Al-Noaimi, I. Warad, Diethylenetriamine/diamines/copper (II) complexes [Cu(dien)(NN)]Br2: Synthesis, solvatochromism, thermal, electrochemistry, single crystal, Hirshfeld surface analysis and antibacterial activity, Arab. J. Chem. 10 (2017) 845–854, doi:10.1016/j.arabjc.2016.10.008.

[48] M.R. Aouad, M. Messali, N. Rezki, N. Al-Zaqri, I. Warad, Single proton intramigration in novel 4-phenyl-3-((4-phenyl-1H-1,2,3-triazol-1-yl)methyl)-1H-1,2,4-

triazole-5(4H)-thione: XRD-crystal interactions, physicochemical, thermal, Hirshfeld surface, DFT realization of thiol/thione tautomerism, J. Mol. Liq. 264 (2018) 621–630, doi:10.1016/j.molliq.2018.05.085.

[49] E. Lindner, S. Al-Gharabli, H.A.Mayera I.Warad, S. Steinbrecher, E. Plies, M. Seiler, H. Bertagnolli, Supported organometallic complexes. XXXVI [1] diaminediphosphine-ruthenium(ii) interphase catalysts for the hydrogenation of α,β-unsaturated ketones, Z. Anorg. Allg. Chem. 629 (2003) 161–171 doi.org/10.1002/zaac.200390010.

[50] A. Shamsi, M. Al Shahwan, S. Ahamad, M.I. Hassan, F. Ahmad, A. Islam, Spectroscopic, calorimetric and molecular docking insight into the interaction of Alzheimer's drug donepezil with human transferrin: implications of Alzheimer's drug, J. Biomol. Struct. Dyn. 38 (2020) 1094–1102, doi:10.1080/07391102.2019.1595728.

[51] K.P. Kepp, Bioinorganic chemistry of Alzheimer's disease, Chem. Rev. 112 (2012) 5193–5239, doi:10.1021/cr300009x.

[52] G. Aljohani, A.A.S. Ali, M.A. Said, D.L. Hughes, S.Y. Alraqa, S. Amran, F. Ahmad, N. Basar, 2-Benzyloxynaphthalene aminoalkylated chalcone designed as acetylcholinesterase inhibitor: Structural characterisation, *in vitro* biological activity and molecular docking studies, J. Mol. Struct. 1222 (2020) 128898, doi:10.1016/j.molstruc.2020.128898.